Superconducting rare earth transition metal borocarbides

H. Rosner, S.-L. Drechsler, S.V. Shulga, K. Koepernik, I. Opahle, H. Eschrig

Institut f. Festkörper- und Werkstofforschung Dresden, D-01171 Dresden, Postfach 270016, Germany

Summary: We present an overview of the present knowledge of the electronic structure of selected properties of quaternary intermetallic rare earth transition metal borocarbides and related boronitride compounds. The calculated highly anisotropic Fermi surfaces exhibit clear similarities such as nested regions but also significant distinctions. Electrons from the nested parts of the Fermi surface affect several properties in the superconducting state. We report theoretical calculations which emphasize the relevance of these electrons to the mechanism of superconductivity. Structural parameters for $ScNi_2B_2C$ derived from total energy calculation allow to discriminate conflicting experimental structural reports. The importance of correlation effects due to the presence of the transition metal component in determining the electronic structure is discussed comparing the band structure calculation results with various electronic spectroscopies such as X-ray absorption spectroscopy (XAS). The excellent agreement with the XAS data suggests a minor importance of correlation effects compared with the cuprate superconductors. Thermodynamic properties of these systems are analyzed within the multi-band Eliashberg theory with special emphasis on the upper critical field $H_{c2}(T)$ and the specific heat. In particular, the unusual positive curvature of $H_{c2}(T)$ near T_c observed for high-quality single crystals, polycrystalline samples of YNi_2B_2C, $LuNi_2B_2C$ as well as to a somewhat reduced extent also for the mixed system $Y_{1-x}Lu_xNi_2B_2C$ is explained microscopically. The values of $H_{c2}(T)$ and of its positive curvature near T_c are intrinsic quantities generic for such samples. Both quantities decrease with growing disorder and thus provide a direct measure of the sample quality.

1 Introduction

Seven years after the discovery [1] of rare earth transition metal borocarbides (nitrides) (RTBC(N)) with T=Ni,Pd,Pt, the place of RTBC(N) compounds within the family of more or less exotic superconductors is still under debate. In contrast to first speculations of a strong similarity to quasi-2D cuprates (suggested by their reminiscent transition metal layered crystal structure), various LDA (local density approximation) band structure calculations performed in 1994/95 (see Refs. 2-14) clearly demonstrated their 3D electronic structure. Finally, the whole class has been classified as traditional intermetallic superconductors, more or less closely related to the A-15's. Only the interplay of antiferromagnetism and superconductivity for R=Ho, Er, Dy, Tm, Tb, Pr has been regarded as a challenging problem

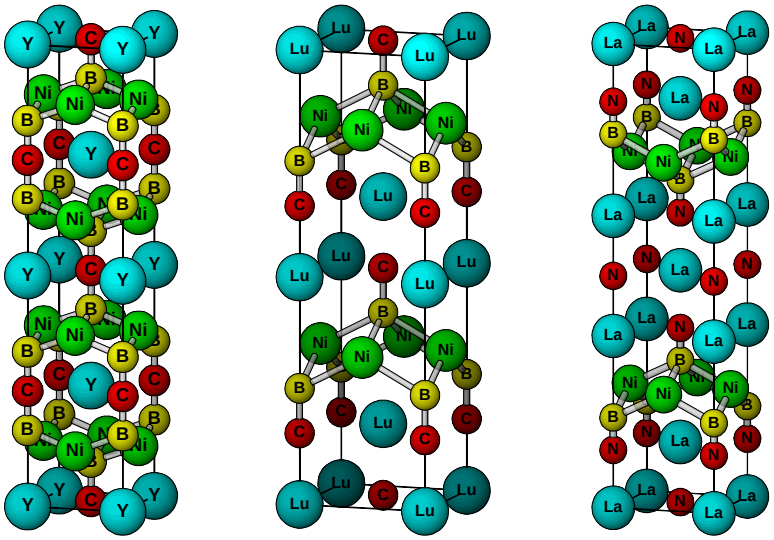

Figure 1 The crystal structure of the single-layer (YNi_2B_2S, left), double-layer (LuNiBC, middle), and triple-layer ($La_3Ni_2B_2N_3$, right) rare-earth transition metal borocarbides, respectively.

of general interest. However, during the last years the situation for non-magnetic borocarbides has been changed considerably as high-quality single crystals have become available revealing (i) more pronounced anisotropies for $LuNi_2B_2C$ [15] (some of them even being strongly temperature dependent) in contrast to the first experimental observations [16] for YNi_2B_2C and (ii) the clear multi-band character of the superconducting state in YNi_2B_2C and $LuNi_2B_2C$ [17]. The crucial importance of such details of the electronic structure, although known in principle from the first calculations, has not been fully appreciated so far. The value of the gap ratio $2\Delta/T_c$, initially fixed to the conventional BCS value 3.5, now varies from 0.45 [18] to 3.2 [19]. Finally, in the context of anisotropy and other unusual properties (see below), d-wave superconductivity has been proposed for YNi_2B_2C and $LuNi_2B_2C$ [20, 21]. Quite interestingly, other RTBC(N) superconductors such as $(LaN)_3(NiB)_2$ show more standard s-wave like behavior [22].

2 Crystal structure and critical temperature

The tetragonal layered crystal structures of the I4/mmm or P4/nmm types resolved so far for all well characterized RTBC(N) compounds can be written schematically as $(RC(N))_n(TB)_2$ with n = 1,2,3 (see Fig. 1). There are empirically discovered systematic dependences of T_c on the T-T distance, the transition metal component, the non-isoelectronic dopants and the B-T-B bond angle. Finally, the

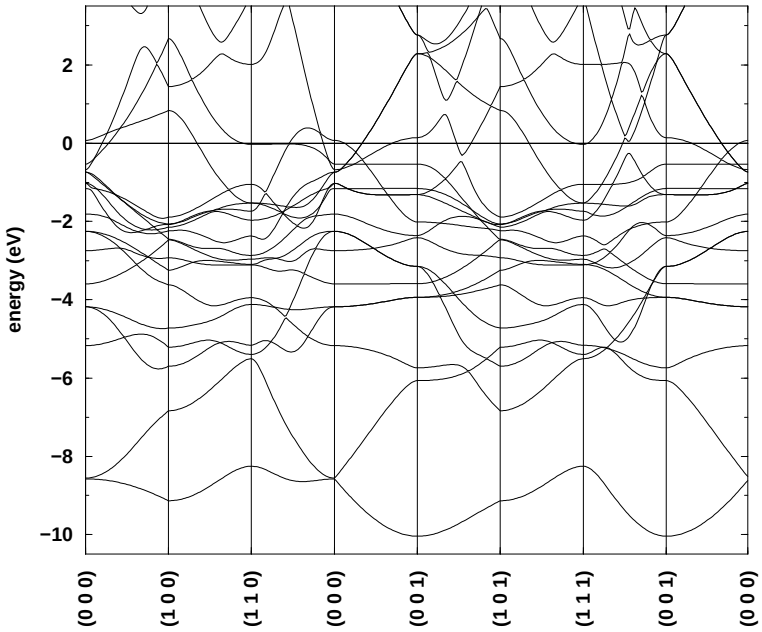

Figure 2 LDA-bandstructure of YNi_2B_2C. The Fermi level is at zero energy. The flat band near the Fermi level between the (110) and (000) points produces the narrow peak in the density of states (see Fig.3).

number of *metallic* layers separating and doping the $(NiB)_2$ networks also has a profound effect on the actual T_c value. Thus, for the single RC-layer (T=Ni) compounds the highest $T_c \approx$14 to 16.6 K values are obtained for R= Sc, Y, Lu, but superconductivity has not been observed so far for R= La. The double-layer Lu- and Y-compounds exhibit very small transition temperatures of 2.9 K and 0.7 K [22], respectively, which however can be increased considerably replacing Ni by Cu [23]. In the case of the two-layer boronitride $(LaN)_2(NiB)_2$ so far no superconductivity has been detected whereas the corresponding triple-layer compound exhibits a relatively high $T_c \approx$ 12K.

3 The electronic structure

A typical bandstructure for a single-layer compound is shown in Fig. 2 for the case of YNi_2B_2C. Similarly, all bandstructure calculations [2-14] for RTBC(N) reveal sizeable dispersion in c-direction of the bands crossing the Fermi level. Electronically the coupling of the 2D-$(TB)_2$ networks is mediated mainly by the carbon and boron $2p_z$ states. Further important issues are the peak of the density of states (DOS) $N(0)$ near the Fermi level E_F=0 (see Fig. 3) and the intermediate strength of correlation effects [24] which is in between the weakly correlated

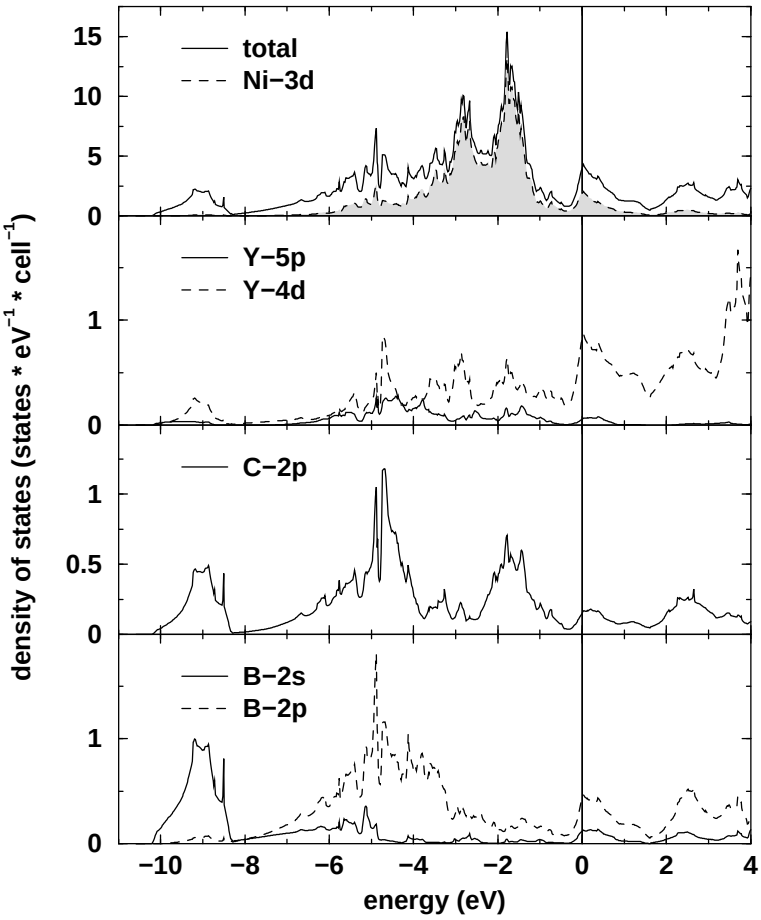

Figure 3 Total as well as partial DOS for YNi_2B_2C. The Fermi level is at zero energy.

Ni-metal and the strongly correlated insulating NiO.

The electronic structure near E_F=0 of all RTBC(N) compounds is characterized by a special band complex containing three bands above about 1eV of the main group of the T-derived *d*-states. For Y(Lu)Ni_2B_2C there is a flat band near E_F (see Fig. 2) giving rise to a narrow asymmetric peak in the total DOS $N(E)$ (see Fig. 3) and to a large T-*d*-partial DOS $N_d(0) \approx 1/2N(0)$ which can be analyzed with high accuracy within our recently developed FPLO-scheme (full-potential non-orthogonal local-orbital minimum-basis scheme) [25]. Compared with Y(Lu)Ni_2B_2C for most of the other RTBC-superconductors $N(0)$ and especially $N_d(0)$ are reduced. However, there is no simple relation between the calculated value of $N(0)$ and the measured T_c-value (see Fig. 4). The comparison with the available specific heat data $c_{p,el} = \gamma T$

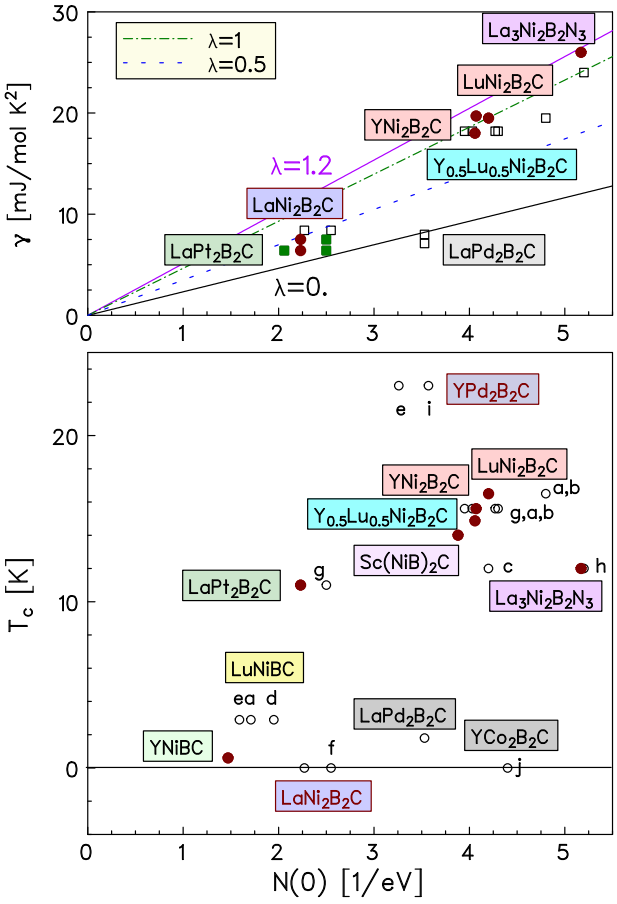

Figure 4 Experimental values of the Sommerfeld constant (top) and the superconducting transition temperature T_c (bottom) *vs.* calculated total density of states at the Fermi level $N(0)$ (states per formula unit) for various RTBC(N)-compounds and different LDA-calculational schemes: Ref. 3-(a), Ref. 2-(b), Ref. 7-(c), Ref. 12-(d), Ref. 10-(e), Ref. 5-(g), Ref. 9-(h), Ref. 6 (i), Ref. 4-(f), Ref. 13-(g), Ref. 9-(h), Ref. 14-(j). .The straight lines in the upper picture denote various *el-ph* coupling constants $0 \leq \lambda \leq 1.2$ (dotted line: λ=0.5, dashed-dotted line: λ=1.0)

$$\gamma = \frac{\pi^2 k_B^2}{3} N(0)\,(1 + \lambda_{el-ph})\,, \tag{3.1}$$

reveals that most RTBC(N)-compounds exhibit intermediately strong averaged electron-phonon (*el-ph*) interaction $\lambda_{el-ph} \sim 0.5$ to 1.2, except $LaPd_2B_2C$ exhibiting extremely weak coupling.

Since polarization dependent x-ray absorption spectroscopy (XAS) probes the unoccupied electronic structure via transitions from the core level into unoccupied states it provides a good opportunity to check the orbital resolved DOS calculated

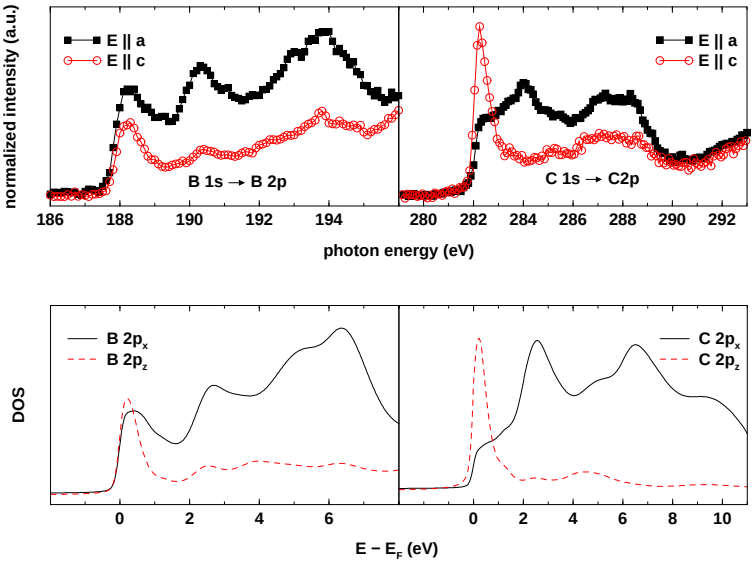

Figure 5 Polarization-dependent XAS spectra ($1s \rightarrow 2p$ transitions) of single crystal YNi_2B_2C are shown for boron (upper left panel) and carbon (uper right panel) with the electric field $\vec{E}$ parallel (open circles) and perpendicular (filled sqares) to the tetragonal c-axis, respectively. The corresponding m-resolved partial DOS from our LDA-FPLO calculations (see text) are denoted by dashed and full lines, and are broadened by account for life time and finite resolution effects.

easily within our FPLO scheme. In particular, for single crystal XAS data of YNi_2B_2C, the transitions from the B(C) $1s$ core level into unoccupied the B(C) $2p_x$ and $2p_z$ states, respectively, are in reasonable agreement with our bandstructure calculation (see Fig. 5)[26].

Many physical properties such as the Hall conductivity, de Haas-van Alphen frequencies and related data, as well as the upper critical magnetical field $H_{c2}(T)$ are strongly dependent on the shape of the Fermi surface and the related Fermi velocity distribution. Our bandstructure predictions for YNi_2B_2C and $LuNi_2B_2C$ are shown in Fig. 7. Both Fermi surfaces exhibit a similar topology, characterized by a strong anisotropic behaviour and special nested regions along the a direction with nesting vectors $\vec{q_n} \sim 0.5$ to $0.6\ 2\pi/a$. However, there are also distinct features for each compound. In particular, their are close and open parts for YNi_2B_2C and $LuNi_2B_2C$, respectively, near $k_z = 0.5\pi/c$. This might explain the qualitative differences between both compounds reported for the Hall data [27] which remained unexplained so far. Nested and anisotropic properties for the Fermi surface of $LuNi_2B_2C$ close to our predictions [28] (see Fig. 6) have been observed by electron-positron annihilation radiation [29].

We emphasize that LDA bandstructure calculations are able to describe with high accuracy various structure related properties such as the lattice constants, the atomic positions, the bulk moduli as well as the frequencies of Raman activ phonon modes. Recently, for the case of $ScNi_2B_2C$, two significantly different structural

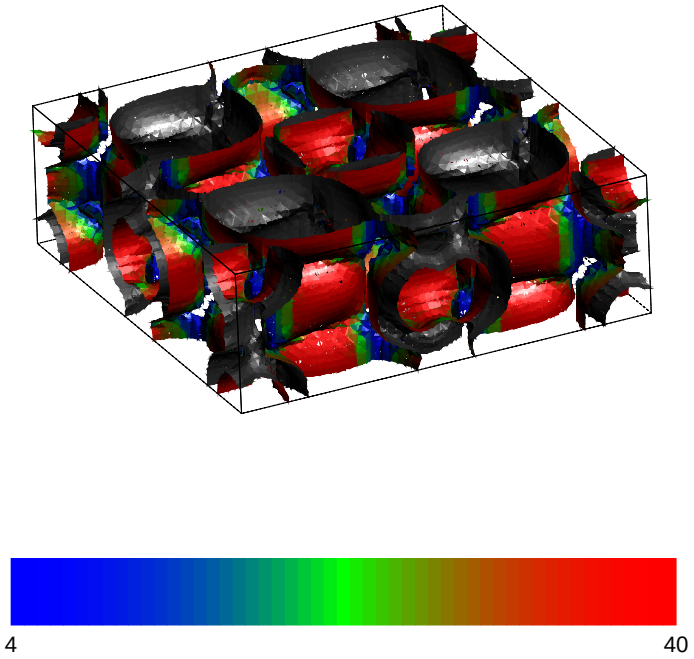

Figure 6 Fermi surface of YNi_2B_2C, the colors corresponds to the Fermi velocities given in a.u.

parameter sets have been reported [30, 31] with c axis lattice constants differing by about 0.5 Å. Assuming the generally accepted I4/mmm space group for this compound, too, we were able to calculate the values for the three independent parameters (unit-cell volume V_0, c/a ratio and boron position) with respect to an minimum of the total energy. The result for V_0 lending strong support for the data of Freudenberger *et al.* [31] and disfavouring the data of Ku *et al.* [30] is shown in Fig. 8. To our knowledge, this is the second remarkable case in the history of the borocarbids research where experimentally determined structural data have been succesfully criticised by LDA bandstructure calculations [32]. In this context we mention that also the experimentally unknown boron position (0,0,z) should be close to our prediction of $z = 0.362$. Experimental data are lacking so far owing to the unsufficient sample quality.

The most valuable insight into the normal state electronic structure can be gained from de Haas-van Alphen (dHvA) measurements[33]. In high-quality YNi_2B_2C single crystals 6 cross sections are observed. The related Fermi velocities $v_{F,i}$, i=1,...,6, on extremal orbits can be grouped into two sets differing by a factor of 4. These observations and the sizable anisotropy of the H_{c2} for such crystals clearly indicate that they are nearly in the clean-limit regime.

To summarize, at the present status, there is a reasonable qualitative agreement between predictions of the LDA-results and experimental data. This points to a

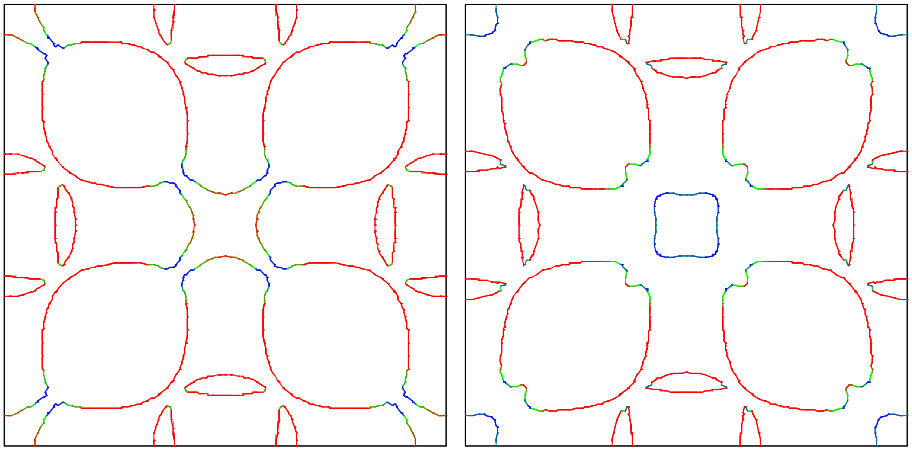

Figure 7 Cuts through the Fermi surface parallel to the (001) plane at the Γ-point for YNi_2B_2C (left panel) and $LuNi_2B_2C$ (right panel). The colors correspond to the Fermi velocities as in Fig. 6

less relevance of correlation effects compared with the high-T_c cuprates.

4 The relationship between the electronic structure and the upper critical field $H_{c2}(T)$

A detailed analysis of the magnitude and the shape of $H_{c2}(T)$ is given in [17]. In particular, the failure of the standard isotropic band approach points to a multi-band description, where electrons with significantly smaller v_F compared with the Fermi surface average (see Fig. 6) $\sqrt{\langle v_F^2 \rangle_{FS}}$ and relatively strong *el-ph* coupling are mainly responsible for the superconductivity. This model explains also approximately the experimentally observed strong deviations of the shape of $H_{c2}(T)$ from the standard parabolic-like curve. In particular, the positive curvature of $H_{c2}(T)$ becomes maximal approaching T_c. All these peculiarities can be described with high accuracy by the simple expression

$$\begin{aligned} H_{c2}(T) &\approx \frac{H_{c2}(0)z}{1-(1+\alpha)tz+L(tz)^2+M(tz)^3}\,, \\ t &= T/T_c \qquad z=(1-T/T_c)^{1+\alpha}. \end{aligned} \tag{4.2}$$

The positive curvature near T_c (characterized by the value of the critical exponent α in Eq. 4.1) has been observed in resistivity, magnetization, and specific heat measurements [28]. This shows unambiguously that the positive curvature is

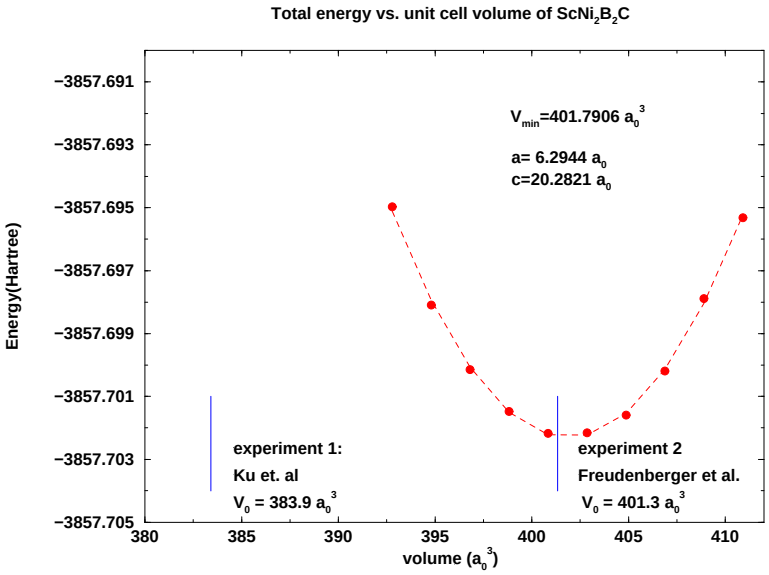

Figure 8 Calculated total energy vs. unit cell volume of $ScNi_2B_2C$ for a fixed c/a ratio and boron position corresponding to the minimum of the total energy found in a self-consistent procedure. The bars denote the two available experimental results.

an inherent thermodynamic property generic for all clean non-magnetic RTBC(N) superconductors.

The saturation (negative curvature) at low T described by the coefficient $L - (1+\alpha)^2 > 0$ is sensitive to details of the Fermi surface and to the value of the smallest of the superconducting gaps.

Together with the second coefficient M it determines the inflection field near $\sim 0.3t$. Thus, a simple but instructive classification of various borocarbide compounds becomes possible. In particular, the nearly triangular shape of H_{c2}(T) for $YC(NiB)_2$ described by large values of L, requires a significantly larger ratio of the fast and slow Fermi velocities v_f compared e.g. with $LuC(NiB)_2$ showing more pronounced parabolic behavior at low T.

In general, the detailed study of different anisotropies with respect to the Fermi surface, to the pairing interaction and possibly also to the order parameter symmetry is the most perspective way to elucidate the mechanism of superconductivity generic for the borocarbides and -nitrides. Obviously, this can be reached only by a strong collaboration of various experimental and theoretical techniques investigating the electronic structure of these fascinating compounds.

The inspection of the distribution of v_F over the Fermi surface of $LuNi_2B_2C$ derived from our FPLO-LDA calculations depicted in Fig. (6). yields that the major part of the electrons (dominating the normal state transport properties) exhibit large v_F-values (red and green) differing up to factor of 6 from the slow electrons (blue). This is in accord with our phenomenological analysis [17] of $H_{c2}(T)$ requiring a factor of at least five in their relative magnitudes. The electrons with low

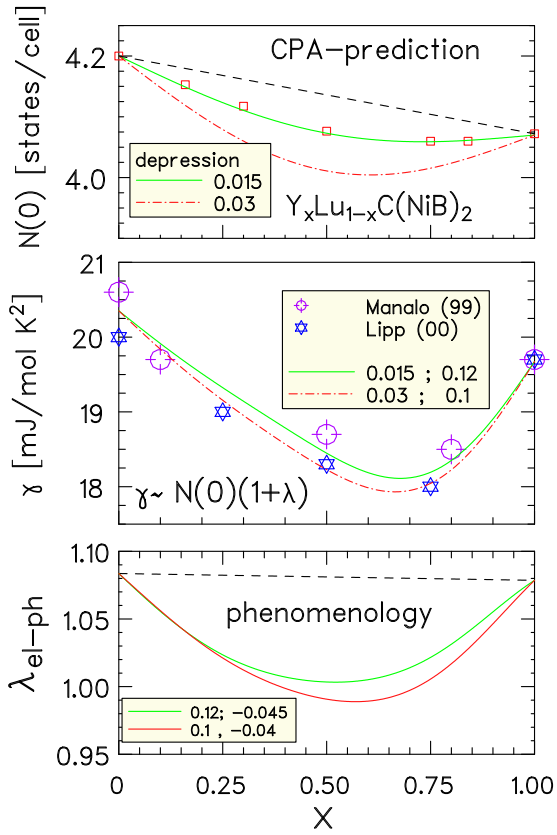

Figure 9 Composition dependence of the DOS at Fermi level $N(0)$ calculated by LDA-CPA (upper panel), the experimental value for the Sommerfeld constant γ (middle panel) and the phenomenologically extracted value of the electron-phonon coupling constant λ (lower panel) for the mixed quasi-quaternary compound $Y_xLu_{1-x}Ni_2B_2C$. The squares in the DOS are self-consistently calculated using the experimental structural data. The dashed-dotted line is an ad-hoc estimate taking into account possible local lattice distortions. The specific heat data are taken from Refs. [37, 38]. The value of the averaged electron phonon coupling constant λ has been derived combining the results for $N(0)$ and γ. The label numbers correspond to the disorder and asymmetry parameter, respectively, analyzed in terms of Eq. (5.3)

.

v_F's are found near nested parts of the Fermi surface. Quite interestingly, vectors closely related to the nesting vector $q \approx 0.6\ 2\pi/a$, i.e. connecting the neighboring blue parts (compare Fig. 6) of Ref. 12), seem to occur also in low-frequency phonons exhibiting anomalously strong softening entering the superconducting state [34] as well as in the incommensurate a-axis modulated magnetic structure which partially suppresses the superconductivity in low magnetic fields [35].

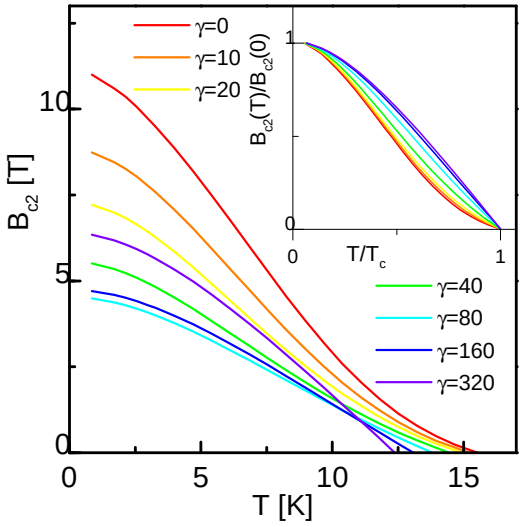

Figure 10 Upper critical field B_{c2} vs. temperature T within the two-band model for various degrees of disorder given by the impurity scattering rate γ (in cm^{-1}). Inset: the same in relative units.

5 Disorder and doping

The generic structure of RTBC(N) compounds exhibits, in spite of the different dimensionality discussed above, a remarkable similarity to the cuprate superconductors with respect to the specific role of the two subsystems comprising these compounds. They consist of the NiB-network which is the stage for the superconducting spectacle and the RC-subsystem playing the role of a charge reservoir. Its main function consists to adjust the Fermi level close to the sharp peak in the DOS (see Fig. 3). For the superconductivity itself it plays a minor active role because of its small admixture to the DOS peak near E_F. Therefore, it can be used to study the effect of disorder in a wide interval. This is of general interest, because these superconductors show anomalous disorder effects. So, the magnitude of $H_{c2}(0)$ and the curvature near T_c of $H_{c2}(T)$ are strongly reduced by disorder (see also Fig.10).

The reduction of the multi-band effects discussed above can be studied by replacing partially some of the constituent atoms by entities with similar chemical and physical properties. Modest effects can be expected for chemically and magnetically equivalent substitutions R $\rightarrow$ R' in the RC(N)-layer(s). For this purpose the crystal structure, T_c, $H_{c2}(T)$, and the electronic specific heat $c_{p,el} = \gamma T$ of the mixed (polycrystalline) $\mathrm{Y}_x\mathrm{Lu}_{1-x}\mathrm{Ni}_2\mathrm{B}_2\mathrm{C}$ system have been studied recently [36, 37, 38]. Since the measured lattice constants a and c vary nearly linearly between the corresponding pure limits, a maximum of T_c might be expected for x=0.5 according to the "universal" curve $T_c = T_c(d_{Ni-Ni})$ proposed by Lai *et al.* [39], where d_{Ni-Ni} denotes the Ni-Ni distance. Instead of the expected maximum

with $T_c \approx 17$ K a sample dependent dip in between x=0.5 to 0.7 with $T_c \approx 14.5$ to 14.9 K has been found.

Several other physical quantities such as the the Sommerfeld constant γ (see Fig. 4), the curvature exponentα of H_c2 exhibit similar dips as a function of the composition [40]. For any physical quantity A from a formal point of view it is convenient to analyze the deviations from the linear interpolation between the border compounds (the so called virtual crystal approximation) by [41] the Fourier components d_m

$$A(x) = (A(0)x + (1-x)A(1)) \left(1 - \sum_m d_m \sin(m\pi x)\right), \tag{5.3}$$

where the strength of the disorder is mainly characterized by the odd components $d_{disorder} = d_1 + d_3 + \ldots$ characterizes whereas the even components describe the disorder induced asymmetry. Analyzing the empirically found dip behavior of the Sommerfeld constant γ (see Eq. (3.1)), the problem about the relative contributions of $N(0)$ and λ_{el-ph} should be addressed. To get some insight in the disorder effects induced by substitutions at T- and R-sites, we performed $N(0)$ calculations for $Lu(Ni_{1-x}Co_xB)_2C$ and $Y_xLu_{1-x}(NiB)_2C$ within the coherent potential approximation (CPA) [42] using the experimentally found linear dependence of the lattice constants upon composition. We found strong effects in the former case whereas in the second case the CPA calculation reveal a very smooth $N(x)$ dependence with a shallow minimum which is approximated by Eq. (5.3) with $d_N \equiv d_1$= 0.015 resulting in $N(x_{min})$ =4.058 states/(eV unit cell) at x_m=0.73 compared with the border values 4.2 at $x = 0$ and 4.072 at $x = 1$. Since in our approach local relaxation have been ignored so far, we admit also a twice as large total value d_N=0.03. Combining our theoretical $N(x)$-dependence with the experimental γ-data we extract the averaged el-ph coupling constant λ. In both cases one arrives at much larger disorder suppressions of λ: $d_\lambda \sim 0.1$ (see Fig. 9, lower panel). Such a disorder suppression of λ is supported also, by the composition dependence of the specific heat jump at T_c [38] which shows a clear disorder induced suppression, too. In particular, even a shallow dip occurs near x=0.4. From a microscopic point of view this should be attributed to a hardening of phonon modes. We speculate that the disorder affects the soft anomalous phonon near 7 meV probably closely related to the Fermi surface nesting discussed above.

The reduction of the positive curvature of H_{c2} points to a direct disorder effect at the level of the superconductivity. It can be described within the framework of the two-band Eliashberg theory admitting significantly increasing effective impurity scattering rates (see Fig. 10). Further experimental support for the presence of such direct disorder effects stems from the electronic specific heat data in the mixed state showing a nonlinear field dependence $c_p \propto T(H/H_{c2})^{1-\beta}$ which vanishes in the dirty limit [38]. In this context recent experimental results of Nohara *et al.* [43, 44] for $Y(Pt_xNi_{1-x})_2C$ single crystals are of considerable interest. According to this data both curvatures (α and β vanish already at $x \sim 0.1$ which clearly indicates the enhanced disorder sensitivity induced by even by isoelectronic substitutions at the T-site compared with our data for the R-site. There at $x = 0.2$ the dirty limit is reached in contrast to the R substitutional case (provided rather similar ionic

radii of the substituted isoelectronic ions as in the Y-Lu case) where the system remains in the quasi-clean limit for any composition.

6 $LuNi_2B_2C$ and YNi_2B_2C: unconventional pairing?

For these two compounds there are several properties which taken together might be interpreted also as hints for unconventional (d-wave or p-wave) superconductivity:
(i) a nonlinear $H^{1-\beta}$-dependence of the electronic specific heat c_{el} in the superconducting state instead of the standard linear dependence,
(ii) the very weak damping of the dHvA oscillations in the superconducting state related to the superconducting gap has been interpreted as strong evidence for a very small or vanishing gap at parts of the Fermi surface [45],
(iii) a non-exponential *non-universal* power-like T-dependence of the electronic specific heat in the superconducting phase $C_{el} \propto T^{\beta}$, $\beta \sim 3$ at low temperatures ($\beta \approx 2.75$ for YNi_2B_2C [46] and $\beta > 3$ for $LuNi_2B_2C$ and $LaPt_2B_2C$). Strictly speaking, a pure one-band d-wave superconductor shows *quadratic* temperature dependence; a cubic dependence is expected for an order parameter with point-like nodes.
(iv) the anisotropy of $H_{c2}(T)$ within the basal plane of $LuNi_2B_2C$ [15] has been ascribed to d-wave pairing [20],
(v) a quadratic flux line lattice at high fields has been observed not only for magnetic RTBC but also for the non-magnetic title compounds[19],
(vi) deviations from the Korringa behavior of the nuclear spin lattice relaxation rate $1/T_1T$=const have been ascribed to the presence of antiferromagnetic spin-fluctuations on the Ni site.

However, it should be noted that several of these unusual properties (i,ii,iii,iv,v) have been observed also for some more or less traditional superconductors such as V_3Si and $NbSe_2$ as well as for heavy fermion superconductors. The possibility of a square flux line lattice for the case of a two-band superconductor has been mentioned by Moskalenko in 1966 [47]. At present it is also unclear to what extent the observed anisotropies and unusual temperature dependences could be described alternatively by a full anisotropic (multi-band) extended s-wave theory. Phase-sensitive experiments [48] and/or the observation of the Andreev bound state near appropriate surfaces[49] must be awaited to confirm or disprove the d-wave scenario.

Most importantly, some of the unusual T-dependences ascribed sometimes to the presence of antiferromagnetic spin fluctuations and "non-Fermi liquid" effects might be caused by the rather strong energy dependence of the DOS near the Fermi level[13]. Finally, the observation of a weak Hebel-Slichter peak in the ^{13}C NMR data for the spin-lattice relaxation time T_1 $(1/T_1T)$ [50] must be mentioned. This points to the presence of at least one s-wave pairing component in the multi-band order-parameter including also the C $2s$-electrons. However, a strong electron-electron interaction is suggested by the twice as large so-called enhancement factor $\alpha_c = 0.6$ compared with those of conventional "s-band" metals Li and Ag.

In this context it should be mentioned that according to our FPLO calculations

the C $2s$ contribution to $N(0)$ is very small ($\leq 1\%$).

7 A possible classification

Bearing the general similarities in the electronic and lattice structures of most RTB(N)-compounds in mind, we propose that essentially the same pairing mechanism should be responsible for all representatives. Since a substantial boron isotope effect has been measured for YNi_2B_2C and due to the absence of conclusive evidence for antiferromagnetic spin-fluctuations [13], the assumption of a dominating *el-ph* mechanism seems to be a quite natural one. In this case, the possible change of the order parameter symmetry (within a part of the multicomponent(band) order parameter) must be ascribed to the Coulomb repulsion. According to [51], increasing for instance the Coulomb pseudopotential μ^*, one approaches a critical ratio μ^*/λ: below and above of which s-wave or d-wave superconductivity occurs, respectively. Due to the minimal extent of the $3d$ Wannier functions, the largest value of the on-site Coulomb interaction U can be expected in the case of the single layer Ni-series. The presence of three intermediate LaN-layers in the triple-compound $(LaN_{1-\delta})_3(NiB)_2$ might contribute to an additional screening of the on-site Coulomb interaction less pronounced in the single-layer compounds. The disorder due to a significant amount of (charged !) N vacancies in the triple layer lantanum boronitride $\delta \sim 0.05$ as well as in T-site substituted single- and two-layer borocarbides might kill any d-wave or highly anisotropic s-wave component present in the clean parent compounds. In this respect the observation of an disorder induced gap in the electronic specific heat of $YC(Pt_xNi_{1-x}B)_2$ in the superconducting state by Nohara *et al.* [44] is quite remarkable. All mentioned above "anomalous" properties are reduced or removed with increasing disorder.

Similarly, the presence of two Lu(Y)C-layers in Lu(Y)NiBC might be helpful to establish superconductivity at least at low temperatures absent in the single-layer compounds $LaNi_2B_2C$, YCo_2B_2C despite their larger $N(0)$-values (see Fig. 3).

In general the understanding of the absence of superconductivity in some of these compounds is of equal importance as the understanding of the representatives with the highest T_c-values. For the $4d$ and $5d$-members of the RTBC-family the DOS near the Fermi level $N(0)$ and especially the partial DOS with d-character $N_d(0)$ are reduced resulting possibly in a reduced Coulomb interaction, too.

The rich variety of superconducting compounds in the novel class of RTBC(N) compounds under consideration and the growing knowledge of their electronic structure offers the fascinating possibility to work out a semi-microscopic quantitative description of these superconductors instead often theories of superconductivity with many adjustable parameters and quantities. This will be helpful to clarify obvious present differences and similarities with other exotic superconductors.

8 Acknowledgment

It is a pleasure to thank G. Fuchs, J. Freudenberger, A. Kreyssig, C. Grazioli, O. Dolgov, and numerous other colleagues for fruitful discussions, collaboration and providing us with experimental data prior to publication. Without the synergetic interaction with them and their stimulating interest the present work would not be possible. We would like to thank also the Deutsche Forschungsgemeinschaft and the Sonderforschungsbereich 463 " Seltenerd-Übergangsmetallverbindungen: Struktur, Magnetismus und Transport" for financial support. Further support by the Graduiertenkolleg "Struktur und Korrelationseffekte in Festkörpern" der TU Dresden is acknowledged (H.R.).

Bibliography

[1] C. Mazumdar *et al.*, Solid State Commun. **87** 413 (1993); R. Nagarajan *et al.*, *Phys.Rev. Lett.* **72**, 274 (1994); R. Cava *et al.*, Nature **376** 146 (1994); ibid. 252 (1994).

[2] W. Pickett and D. Singh, Phys. Rev. Lett. **72** 3702 (1994).

[3] L.F. Mattheiss, Phys. Rev. B **49** 13 279 (1994).

[4] L.F. Mattheiss *et al.*, Solid State Commun. **91** 587 (1994).

[5] D. Singh, Phys. Rev. B **50** 6486 (1994).

[6] W. Pickett and D. Singh, J. of Supercond. **8** (1995) 425.

[7] D. Singh and W. Pickett, Phys. Rev. B **51** 8668 (1995).

[8] D. Singh, Solid State Commun. **98** 899 (1995).

[9] L.F. Mattheiss, Solid State Commun. **94** 741 (1995).

[10] R. Coehoorn, Physica C **228** 331 (1994).

[11] R.Y. Rhee *et al.*, Phys. Rev. B **51** 15585 (1995) .

[12] H. Kim *et al.*, Phys. Rev. B **52** 4592 (1995).

[13] B.J. Suh *et al.* , Phys. Rev. B **53** R6022 (1996).

[14] P. Ravindran *et al.*, Phys. Rev. B **58** 3381 (1998).

[15] V. Metlushko *et al.*, Phys. Rev. Lett. **79** 1738 (1997).

[16] M. Xu *et al.*, Physica C **235** 2533 (1994).

[17] S.V. Shulga *et al.*, Phys. Rev. Lett. **80** 1730 (1998).

[18] T. Jacobs *et al.*, Phys. Rev. B **52** R7022 (1995).

[19] Y. de Wilde *et al.*, Phys. Rev. Lett. **78** 4273 (1997); R. Eskildsen *et al.*, ibid. **79** 487 (1997); M. Yethiraj *et al.*, ibid. **78** 4849 (1997).

[20] G. Wang and K. Maki , Phys. Rev. B, **58** 6493 (1998).

[21] M. Nohara *et al.*, J. Phys. Soc. Jpn. **66** 1888 (1997); R. Takagi *et al.* Physica B **237-238** 292 (1997).

[22] G. Hilscher and H. Michor, in "Studies of High Temperature Superconductors" (Ed. A.V. Narlikar), Nova Science Publishers, N.Y. v. **26/27** (1998).

[23] A.K. Gangopadhyay and J.S. Schilling , Phys. Rev. B **54** 10 107 (1996).

[24] T. Böske *et al.*, Solid State Commun. **98** 813 (1996).

[25] K. Koepernik and H. Eschrig, Phys. Rev. B, **59** 1743 (1999).

[26] H. Lips *et al.*, Phys. Rev. B, **60** 11144 (1999).

[27] V.N. Narozhnyi *et al.*, Phys. Rev. B, **59**, 14762 (1999).

[28] S.-L. Drechsler *et al.*, Physica C, **317-318**, 117 (1999).

[29] S.B. Dugdale *et al.*, Phys. Rev. Lett., **83**, 4824 (1999).

[30] H.C. Ku *et al.*, Phys. Rev. B, **50**, 351 (1994).

[31] J. Freudenberger, "Paarbrechung in Seltenerd-Übergangsmetall-Borkarbiden" Dissertation, TU Dresden, (2000)

[32] D. Singh and W.E. Pickett, Nature **374** , 682 (1995).

[33] L.H. Nguyen *et al.*, J. Low Temp. Phys., **105**, (1996) 1653.

[34] C. Stassis *et al.*, Physica C **317-318** 127 (1999); M. Bullock *et al.* Phys. Rev. B **57** 7916 (1998).

[35] K.-H. Müller *et al.*, J. Appl. Phys. **81** 4240 (1997).

[36] J. Freudenberger *et al.*, Physica C **306** 1 (1998).

[37] S. Manalo *et al.*, preprint cond.-mat/9911305 (1999).

[38] D. Lipp *et al.*, to be published.

[39] C. Lai *et al.*, Phys. Rev. B **51** 420 (1995).

[40] S.L. Drechsler *et al.*, Physica C (in press).

[41] S.L. Drechsler *et al.*, J. Low Temp. Phys., **117**, 1617 (1999).

[42] K. Koepernik *et al.*, Phys. Rev. B, **55**, 5717 (1997).

[43] M. Nohara, M. Isshiki, F. Sakai, H. Takagi, J. Phys. Soc. Jpn. **68**, 1078 (1999).

[44] M. Nohara, H. Suzuki, N. Mangkorntong, and H. Takagi, Proceedings of M^2S-HTSC, Houston 20-25.2. 2000, Physica C, in press (2000).

[45] T. Terashima *et al.*, Phys. Rev. B **56**, 5120 (1997).

[46] N.M. Hong *et al.*, Physica C **227**, 85 (1994).

[47] V.A. Moskalenko, ZhETF, **51**, 1163 (1966).

[48] D.A. Wollman *et al.* Phys. Rev. Lett. **71**, 2134 (1993).

[49] C.-R. Hu, Phys. Rev. Lett. 72, 1526 (1994).

[50] T. Saito *et al.* , J. Magn. and Magnetic Materials, **177-181**, 557 (1998).

[51] G. Varelogiannis, Phys. Rev. B **57**, 13743 (1998).